



# Low particulate organic carbon export in the frontal zone of the Southern Ocean (Indian sector) revealed by $^{234}\text{Th}$

L. Coppola<sup>a,b,\*</sup>, M. Roy-Barman<sup>a,c</sup>, S. Mulsow<sup>d</sup>, P. Povinec<sup>d</sup>, C. Jeandel<sup>a</sup>

<sup>a</sup>LEGOS, 14 avenue, Edouard Belin 31400 Toulouse, France

<sup>b</sup>LIG, Swedish Museum of Natural History, Box 50007, 104 05 Stockholm, Sweden

<sup>c</sup>LSCE, Avenue de la Terrasse, 91198 Gif sur Yvette, France

<sup>d</sup>IAEA-Marine Environment Laboratory, 4 quai Antoine 1er, MC 98000, Monaco

Received 2 April 2003; received in revised form 26 January 2004; accepted 23 July 2004

## Abstract

The water column deficiencies of  $^{234}\text{Th}$  were used to estimate the Particulate Organic Carbon (POC) fluxes in the Indian Sector of the Southern Ocean. Samples were collected in January–February 1999 in a frontal zone from 42°S to 47°S and from 60°E to 66°E during the ANTARES 4 cruise. Beta counting was used to measure the  $^{234}\text{Th}$  activities onboard. The  $^{234}\text{Th}$  export fluxes were estimated from the  $^{234}\text{Th}/^{238}\text{U}$  disequilibria using a steady state  $^{234}\text{Th}$  model. A non-steady state model gave results close to the steady-state model in the Subtropical Zone and could not be used in the Subantarctic Zone due to a strong vertical mixing event. Small and large particles analysis indicated that the  $\text{POC}/^{234}\text{Th}$  ratios decreased when the particle size increased. From the  $\text{POC}/^{234}\text{Th}$  ratios on the large filtered particles, it appears that the POC export fluxes exported below 100 m were very low (from 0.10 to 2.53  $\text{mmolC m}^{-2} \text{d}^{-1}$ ) compared to those observed in the Southern Ocean and (Deep Sea Res. II 48 (2001) 4275; Deep Sea Res. II 47 (15–16) (2000) 3451; Deep Sea Res. II 44 (1997) 457) and with a strong zonal variation. It is hypothesized that the low POC export fluxes were related to the low predominance of diatoms, characteristic at the end of a bloom period. In this way, the very low POC export observed in the Subtropical Zone suggests an efficient remineralization process and/or a high bacterial activity. Otherwise, a decoupling between the primary production and the POC export derived from  $^{234}\text{Th}$  could also explain the low POC export.

© 2004 Elsevier Ltd. All rights reserved.

*Keywords:* Thorium-234; POC export; Southern Ocean

## 1. Introduction

The Southern Ocean plays a major role in the global climate change since it is considered to be an important sink of atmospheric  $\text{CO}_2$ . For

\*Corresponding author. Tel.: +46 8 5195 4234;  
fax: +46 8 5195 4031.

E-mail address: [laurent.coppola@nrm.se](mailto:laurent.coppola@nrm.se) (L. Coppola).

example, the Subantarctic sector of the Southern Ocean adsorbs up to 1 Gt C/y (Metzl et al., 1999) and the Southern Ocean (south of 30°S) contributes about 30% of the total export flux of particulate carbon (Schiltzer, 2002). This region is characterized as the largest High-Nutrient and Low-Chlorophyll (HNLC) area of the world ocean with elevated productivity being only observed in the Polar Front due to the entrainment of trace elements (De Baar et al., 1995). Recently, several studies (e.g. SOIREE) have suggested that increasing the supply of iron to the Southern Ocean would lead to enhanced uptake of atmospheric CO<sub>2</sub> and sequestration of carbon via sinking particles. However, no increase of the Particulate Organic Carbon (POC) export was observed during these experiments. These studies demonstrated that iron supply controls phytoplankton growth but that carbon sequestration remains poorly constrained and depends on the processes controlling export and remineralization of carbon (Boyd et al., 2000).

In this paper, we study the rate of carbon export in the Indian sector of the Southern Ocean. The oceanographic setting is quite different from the rest of the Subantarctic Southern Ocean. In this region, the Subantarctic and Subtropical Fronts converge, constrained by the Kerguelen Plateau in the south and the Agulhas Return Current Front in the north (Park et al., 1993; Park and Gamberoni, 1997). The fourth part of the French Joint Global Ocean Flux Study (JGOFS) ANTARctic RESEARCH program (ANTARES 4) aimed to quantify the stock and the export of biogenic particles fluxes (C, N, Si) in relation to the biological pump of the atmospheric CO<sub>2</sub> in the Indian sector of the Southern Ocean. The sampling zone of ANTARES 4 was characterized by a frontal zone located in the north of the Crozet basin, one of the most dynamic areas of the Southern Ocean (Park and Gamberoni, 1995). In this study area, three fronts strongly converged around the Crozet-Kerguelen basin: Subantarctic Front (SAF), Subtropical Front (STF) and Agulhas Return Current (AF). This zone is characterized by transition from cold, nutrient-rich polar waters to warm, nutrient-poor subtropical waters that

occurs over a narrow latitudinal range of several degrees (Sedwick et al., 2002).

In the open ocean, the main source of particles is biological production, which varies with space and time. Organic particles are produced from carbon fixation through photosynthesis and uptake of nutrients (primary production). Most of the POC is recycled in the surface water by decomposition to dissolved organic carbon and remineralization/respiration to inorganic carbon. Only a small fraction of POC is exported from the euphotic layer and subsequently either recycled in the deep waters or reaching the sediments. The large particles, which have high settling velocity (diatoms, aggregates, fecal pellets), are responsible for the vertical POC fluxes. The POC export out of the surface layer is the most important biological process for the transport of the atmospheric CO<sub>2</sub> to the deep ocean when the phytoplankton is large in size (Trull et al., 2001).

The natural radionuclide <sup>234</sup>Th is produced in situ from decay of dissolved <sup>238</sup>U, which is conservative with salinity. In seawater, <sup>234</sup>Th is insoluble, very reactive and present in different forms: dissolved, colloidal or attached on small and large particles (Baskaran et al., 2003). Its short half-life (24.1 d) is appropriate to quantify particles processes on time scales of days to weeks. In the surface ocean, the deficit of <sup>234</sup>Th with respect to <sup>238</sup>U is currently used to quantify the rate of particle export from the euphotic zone (Coale and Bruland, 1987; Murray et al., 1989; Buesseler et al., 1992). In Southern Ocean, the proxy <sup>234</sup>Th has been used to obtain export rates of POC (Buesseler et al., 2001; Cochran et al., 2000; Rutgers van der Loeff et al., 1997).

## 2. Sampling and analytical methods

### 2.1. Study area

The ANTARES 4 cruise was conducted aboard RV Marion Dufresne II in the Crozet basin during January and February 1999. The sampling zone was located northwest of Kerguelen Islands in an area bounded by 42–47°S and 60–66°E where the confluence of the SAF and STF was aligned in a

southwest to northeast direction (Park et al., 2002; Fig. 1). The identified mesoscale structures allowed to locate three long stations (more or less 4 days

for each station) measured in Lagrangian mode following a drifting buoy connected to sediment traps deployed at 200 m below the surface. These

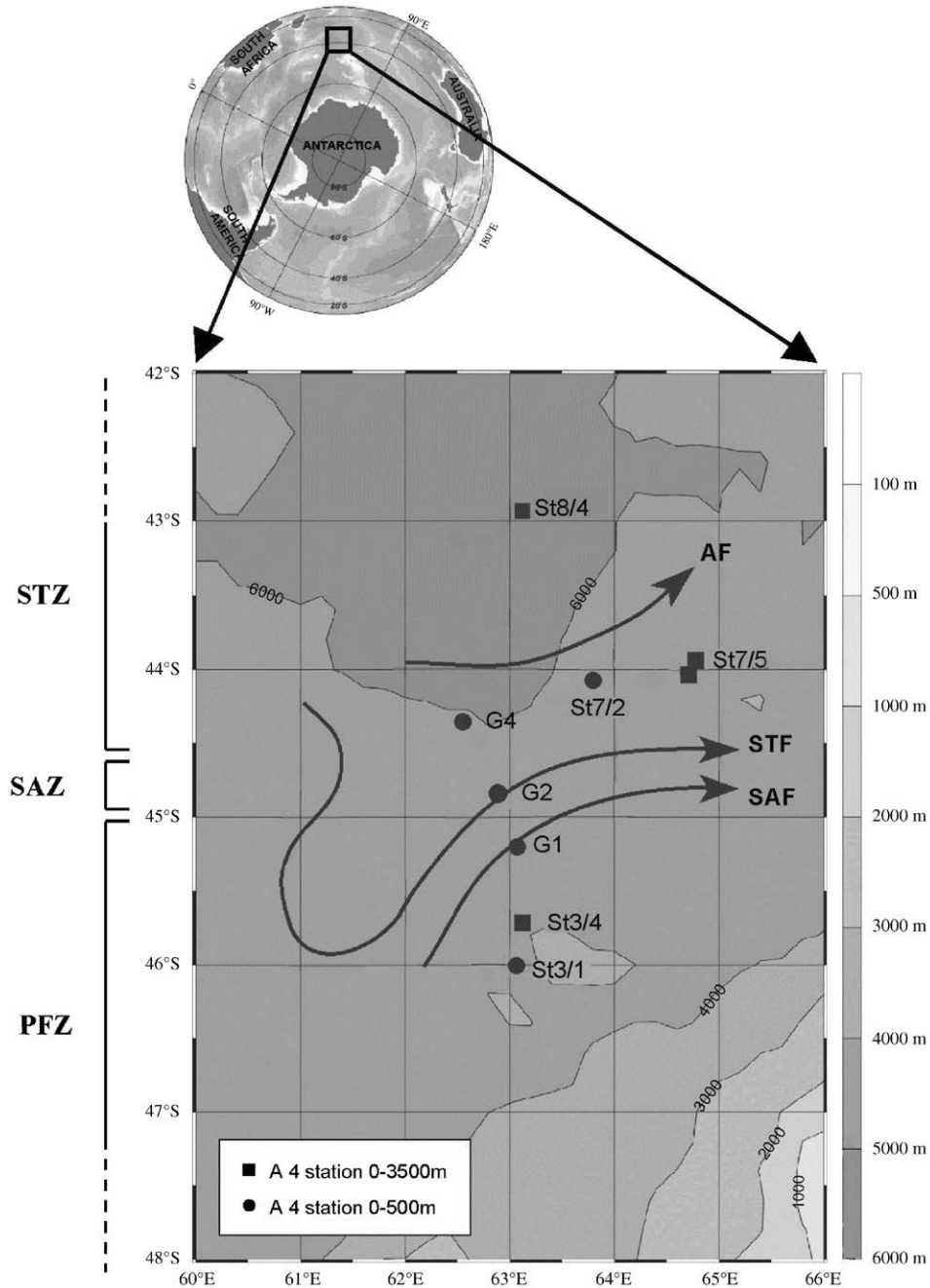


Fig. 1. Map of the ANTARES 4 study area. Location of sampling stations and position of hydrological fronts (SAF: Subantarctic Front; STF: Subtropical Front; AF: Agulhas return current; Park et al., 2002).

stations were studied for production and export processes of biogenic matter and sampled at depths ranging from 10 to 3500 m. The southernmost (station 3) was positioned in the Polar Front Zone (PFZ with high levels of N, P and low levels of Si), station 7 was located in the frontal area between the AF and STF, and the northernmost (station 8), was chosen in the subtropical oligotrophic waters (low levels of N, P and Si) influenced by the AF. For station 3 and 7, samples were collected twice: St3/1 and St3/4 (first and fourth day) and St7/2 and St7/5 (second and fifth day). At station 8, samples were collected only on the fourth day. During the sampling cruise, three short stations (4 h) were located on the CTD and TOWYO transects (G1, G2, and G4) to measure the export production from the euphotic layer and were sampled at depths ranging from 10 m to 500 m.

## 2.2. Materials and methods

During the ANTARES 4 cruise,  $^{234}\text{Th}$  activities in the water column were measured by beta and gamma counting. In the present study, we will focus on the beta counting data used to estimate the vertical particulate  $^{234}\text{Th}$  and POC fluxes from the euphotic zone in the Indian sector of the Southern Ocean.

### 2.2.1. Dissolved and small particulate phases

In order to measure  $^{230}\text{Th}$  and  $^{232}\text{Th}$  as well as  $^{234}\text{Th}$ , we used a pre-concentration method first developed to evaluate  $^{230}\text{Th}$  and  $^{232}\text{Th}$  by Thermal Ionization Mass Spectrometry (TIMS; Roy-Barman et al., 1996; Coppola et al., 2003). Seawater samples were collected with Niskin bottles connected to the CTD instruments and immediately filtered through acid-washed  $0.6\ \mu\text{m}$  Nuclepore<sup>®</sup> polycarbonate membrane filters using a Millipore<sup>®</sup> filtration system. Around 20–30 l of seawater were used to measure the small particulate fraction of  $^{234}\text{Th}$  ( $>0.6\ \mu\text{m}$ ). All filtered seawater samples were acidified to pH 2 with 18 ml distilled HCl 6N per 10 l of sample to avoid thorium absorption on bottles wall. A  $^{229}\text{Th}$  yield tracer and Fe carrier were added to the filtered seawater. For all samples, the iron precipitation was done 1–2 days after the sample collection. After an

overnight of isotopic equilibration, pH was raised to 8 with  $\text{NH}_4\text{OH}$  solution (25%) to scavenge dissolved Th on  $\text{Fe}(\text{OH})_3$  particles (Roy-Barman et al., 1996). After 24 h of mixing, the precipitate was filtrated through another  $0.6\ \mu\text{m}$  Nuclepore<sup>®</sup> filter. These second filters were used to measure the dissolved fraction of  $^{234}\text{Th}$  (Coppola et al., 2002).

### 2.2.2. Large particulate phase

Large particles were collected with in situ pumps (MARK II, Challenger Oceanic) at each long station at depths ranging from 30 to 2400 m. A large volume of seawater (500–2000 l) was filtered through 143 mm diameter and  $60\ \mu\text{m}$  mesh Teflon filters. For each sample a fraction was used for the POC analysis (in cooperation with R. Sempère) and another for the  $^{234}\text{Th}$  beta counting. The large particulate matter used to measure the  $^{234}\text{Th}$  activities was washed off the filters with pH 8 Milli-Q water (seawater pH). This solution was filtered through  $0.6\ \mu\text{m}$  Nuclepore<sup>®</sup> filters. For the POC analysis, seawater was used for particle removal and dilution (Panagiotopoulos et al., 2002).

## 2.3. $^{234}\text{Th}$ analysis

After the sampling, all filters (containing particulate and precipitate) were dried and folded to produce  $18 \times 18\ \text{mm}^2$  packages which were wrapped in thin polyester or polyethylene plastic foil (Rutgers van der Loeff and Moore, 1999). These filters were analyzed onboard for  $^{234}\text{Th}$  by non-destructive beta counting (Riso National Laboratory). In the open ocean,  $^{234}\text{Th}$  activity usually overwhelms other radionuclides (such as  $^{40}\text{K}$  and  $^{226}\text{Ra}$  decay products) that might contribute to the beta signal from suspended particles. To check this, we followed the decay of  $^{234}\text{Th}$  in samples over several months. Five months later, we again measured the filter background and we determined individually each filter's absorption with uranium standard (work done at the International Atomic Energy Agency's Marine Environment Laboratory in Monaco IAEA-MEL). It was calculated that self-absorption of filters containing iron precipitate and particles from samples reduced their count rates by 30% and 20%, respectively. The beta counter was calibrated

using a  $^{238}\text{U}$  standard and blanks (filters and iron). The counting time was a  $10 \times 100$  min cycle.

However, we did not recover all the  $\text{Fe}(\text{OH})_3$  precipitate because it clogged the filter before the end of filtration. Therefore, only 50% of the precipitate solution was recovered. To correct for the chemical recovery and the amount of  $^{234}\text{Th}$  contributed from the ingrowth of  $^{234}\text{Th}$  from the co-precipitated  $^{238}\text{U}$ , each precipitate containing the dissolved  $^{234}\text{Th}$  fraction was dissolved in distilled 6 N HCl and the solution was divided into 3 fractions: one for the precipitation yield measurement (20% of the volume), one for  $^{238}\text{U}$  determination (10% of the volume) and the remaining was used for the  $^{230}\text{Th}$ – $^{232}\text{Th}$  analysis (Coppola et al., 2003). For the first aliquot, a known quantity of  $^{232}\text{Th}$  standard was added. After isotopic equilibration, this solution was passed through anionic ion exchange columns (Biorad<sup>®</sup>) to extract Th isotopes for measuring the  $^{229}\text{Th}/^{232}\text{Th}$  ratios by Thermal Ionization Mass Spectrometry (TIMS-MAT 261). Knowing the quantity of  $^{232}\text{Th}$  added to the aliquot, it was possible to calculate the amount of  $^{229}\text{Th}$  in the precipitate and the precipitate filtration yield. Furthermore, to correct the dissolved  $^{234}\text{Th}$  activities of additional decay from  $^{238}\text{U}$ , we applied two  $^{234}\text{Th}$  ingrowth corrections. First, we estimated the amount of  $^{234}\text{Th}$  produced between sample collection and  $\text{Fe}(\text{OH})_3$  precipitation. This ingrowth represents from 3% to 6% of the  $^{234}\text{Th}$  dissolved activity. The second correction corresponds to the amount of  $^{234}\text{Th}$  produced by the  $^{238}\text{U}$  scavenged by the iron precipitate and contained on the dissolved fraction filters. The amount of  $^{238}\text{U}$  in the precipitate was measured by Inductively Coupled Plasma-Mass Spectrometry (ICP-MS) on the second aliquot taken after dissolution of the filters. It represents at most 5% of the  $^{238}\text{U}$  concentration in the seawater. Taking into account the time delay between the iron precipitate filtration and the filter beta counting (2–4 d), the second  $^{234}\text{Th}$  correction represents only 0.3–0.6% of the dissolved  $^{234}\text{Th}$  activity. The uncertainties introduced by these corrections were included in the total uncertainties of the dissolved  $^{234}\text{Th}$  activities that represent 7–15%. Typical blanks were  $^{234}\text{Th}=0.5$  cpm

(blank average correction=8%) for filter and  $^{234}\text{Th}=1.9$  cpm (blank average correction=30%) for iron precipitate.

### 3. Results

$^{234}\text{Th}$  results in dissolved and on small ( $>0.6 \mu\text{m}$ ) and large ( $>60 \mu\text{m}$ ) particulate phases are listed in Table 1 and shown in Fig. 2. The  $^{238}\text{U}$  concentrations were calculated using the relationship  $^{238}\text{U}$  (dpm/l) =  $0.071 \times \text{salinity}$  (Chen et al., 1986). The  $^{234}\text{Th}$  activities on large particles were lower than those measured on small particles and the lowest concentrations were observed at station 3. Particulate  $^{234}\text{Th}$  activities decreased with depth and varied significantly with the station positions. They were relatively lower in the PFZ (0.4–0.5 dpm/l) than those measured in the STZ (1–1.3 dpm/l). For all stations, the small particulate  $^{234}\text{Th}$  activities and the fluorescence values were at a maximum at the same depth (between 30 and 50 m).

The total  $^{234}\text{Th}/^{238}\text{U}$  ratio was used to evaluate the particulate  $^{234}\text{Th}$  export. In general, the values were lower than 1 in surface waters ( $^{234}\text{Th}/^{238}\text{U}$  disequilibrium) and close to 1 in the deeper waters ( $^{234}\text{Th}/^{238}\text{U}$  equilibrium). In the PFZ, total  $^{234}\text{Th}/^{238}\text{U}$  ratios ranged from 0.26 to 1.2 between 0 and 500 m depth with an excess at 100 m depth for St3/4. Below the photic zone, total  $^{234}\text{Th}/^{238}\text{U}$  ratios reached the equilibrium except at St3/4 where values were constant and close to 0.7 (Table 1). In the STZ, we observed a  $^{234}\text{Th}/^{238}\text{U}$  disequilibrium in the upper layer. The  $^{234}\text{Th}/^{238}\text{U}$  equilibrium was reached around 200 m depth and we observed an excess at 1500 m depth for St7/5 and St8/4 (Table 1). At deeper depths, the  $^{234}\text{Th}/^{238}\text{U}$  equilibrium was reached again.

### 4. Discussion

#### 4.1. $^{234}\text{Th}/^{238}\text{U}$ disequilibrium in deep water at station 3

Usually, in the deep waters, the total  $^{234}\text{Th}$  activity is expected to be in secular equilibrium

Table 1  
 $^{234}\text{Th}$  activities in dissolved (d), small and large particulate (p and l) phases.

Depth (m)	$^{234}\text{Th}_d \pm 1\sigma < 0.6 \mu\text{m}$ (dpm/l)	$^{234}\text{Th}_p \pm 1\sigma > 0.6 \mu\text{m}$ (dpm/l)	$^{234}\text{Th}_l \pm 1\sigma$ (dpm/l)	$^{238}\text{U}$ (dpm/l)	$^{234}\text{Th}/^{238}\text{U} \pm 1\sigma$ (dpm/dpm)	$^{234}\text{Th}_l \pm 1\sigma > 60 \mu\text{m}$ (dpm/ $10^3\text{l}$ )
St3/1 (#OPA003, 46.01°S, 63.06°E, 4251 m) <sup>a</sup>						
10	0.25 ± 0.17	0.38 ± 0.01	0.63 ± 0.17	2.39	0.26 ± 0.07	
50	1.37 ± 0.17	0.38 ± 0.01	1.75 ± 0.17	2.39	0.73 ± 0.07	
100	2.30 ± 0.16	0.14 ± 0.00	2.44 ± 0.16	2.40	1.02 ± 0.07	
200	2.31 ± 0.17	0.10 ± 0.00	2.41 ± 0.17	2.41	1.00 ± 0.07	
500	2.18 ± 0.17	0.09 ± 0.00	2.27 ± 0.17	2.43	0.93 ± 0.07	
St3/4 (#OPA077, 45.66°S, 63.11°E, 4320 m) <sup>a</sup>						
10	1.00 ± 0.18	0.41 ± 0.01	1.41 ± 0.18	2.39	0.59 ± 0.07	
30	1.52 ± 0.16	0.52 ± 0.03	2.03 ± 0.17	2.39	0.85 ± 0.07	
50	1.38 ± 0.15	0.37 ± 0.01	1.74 ± 0.15	2.39	0.73 ± 0.06	
100	2.77 ± 0.16	0.15 ± 0.01	2.92 ± 0.16	2.40	1.22 ± 0.07	8.44 ± 0.11
200	1.89 ± 0.17	0.39 ± 0.02	2.28 ± 0.17	2.41	0.95 ± 0.07	
500	2.44 ± 0.17	0.09 ± 0.01	2.54 ± 0.17	2.43	1.04 ± 0.07	
1000	—	—	—	—	—	0.53 ± 0.07
1500	1.68 ± 0.17	0.09 ± 0.00	1.77 ± 0.17	2.46	0.72 ± 0.07	5.13 ± 0.51
2500	1.66 ± 0.16	0.05 ± 0.00	1.71 ± 0.16	2.47	0.69 ± 0.06	0.77 ± 0.30
3000	—	0.13 ± 0.01	—	2.47	—	
3500	1.72 ± 0.16	0.07 ± 0.00	1.78 ± 0.16	2.46	0.72 ± 0.06	
G1 (#OPA097, 45.19°S, 63.08°E, 4731 m) <sup>b</sup>						
10	1.40 ± 0.21	0.32 ± 0.02	1.73 ± 0.21	2.39	0.72 ± 0.09	
50	1.15 ± 0.18	0.34 ± 0.02	1.49 ± 0.18	2.39	0.62 ± 0.07	
80	1.20 ± 0.16	0.27 ± 0.02	1.47 ± 0.16	2.40	0.61 ± 0.07	
200	1.87 ± 0.17	0.11 ± 0.01	1.98 ± 0.17	2.41	0.82 ± 0.07	
500	2.02 ± 0.17	0.16 ± 0.01	2.19 ± 0.18	2.43	0.90 ± 0.07	
G2 (#OPA105, 44.84°S, 62.88°E, 4731 m) <sup>b</sup>						
10	0.96 ± 0.18	1.14 ± 0.06	2.10 ± 0.19	2.42	0.87 ± 0.08	
35	1.34 ± 0.17	1.22 ± 0.06	2.55 ± 0.18	2.42	1.05 ± 0.07	
50	1.05 ± 0.15	1.02 ± 0.05	2.07 ± 0.16	2.42	0.85 ± 0.07	
200	2.67 ± 0.17	0.19 ± 0.01	2.86 ± 0.17	2.46	1.16 ± 0.07	
500	2.70 ± 0.17	0.15 ± 0.01	2.85 ± 0.17	2.44	1.17 ± 0.07	
G4 (#OPA124, 44.33°S, 62.53°E, 4928 m) <sup>b</sup>						
10	1.33 ± 0.16	1.02 ± 0.05	2.35 ± 0.17	2.45	0.96 ± 0.07	
30	0.96 ± 0.15	0.94 ± 0.04	1.90 ± 0.16	2.45	0.78 ± 0.07	
100	2.54 ± 0.16	0.37 ± 0.02	2.91 ± 0.16	2.48	1.17 ± 0.06	
200	2.38 ± 0.20	0.19 ± 0.01	2.57 ± 0.20	2.47	1.04 ± 0.08	
500	2.23 ± 0.19	0.16 ± 0.01	2.40 ± 0.19	2.46	0.97 ± 0.08	
St7/2 (#OPA168, 44.07°S, 63.73°E, 4928 m) <sup>c</sup>						
10	1.00 ± 0.15	1.26 ± 0.03	2.26 ± 0.16	2.44	0.93 ± 0.06	
35	0.84 ± 0.15	1.11 ± 0.03	1.95 ± 0.15	2.44	0.80 ± 0.06	
100	1.76 ± 0.14	0.18 ± 0.01	1.95 ± 0.14	2.49	0.78 ± 0.06	
200	2.20 ± 0.15	0.11 ± 0.01	2.31 ± 0.15	2.48	0.93 ± 0.06	
500	2.17 ± 0.16	0.11 ± 0.01	2.28 ± 0.16	2.46	0.93 ± 0.07	
St7/5 (#OPA240/244, 44.01°S, 64.73°E, 4798 m) <sup>c</sup>						
10	0.93 ± 0.15	0.99 ± 0.03	1.92 ± 0.16	2.44	0.79 ± 0.06	
40	0.81 ± 0.14	0.91 ± 0.02	1.72 ± 0.15	2.44	0.71 ± 0.06	30.43 ± 0.33
100	2.06 ± 0.14	0.32 ± 0.01	2.37 ± 0.14	2.48	0.96 ± 0.06	6.68 ± 0.08
200	2.16 ± 0.15	0.15 ± 0.01	2.32 ± 0.15	2.48	0.94 ± 0.06	31.05 ± 0.96

Table 1 (continued)

Depth (m)	$^{234}\text{Th}_d \pm 1\sigma < 0.6 \mu\text{m}$ (dpm/l)	$^{234}\text{Th}_p \pm 1\sigma > 0.6 \mu\text{m}$ (dpm/l)	$^{234}\text{Th}_t \pm 1\sigma$ (dpm/l)	$^{238}\text{U}$ (dpm/l)	$^{234}\text{Th}/^{238}\text{U} \pm 1\sigma$ (dpm/dpm)	$^{234}\text{Th}_t \pm 1\sigma > 60 \mu\text{m}$ (dpm/10 <sup>3</sup> l)
500	2.31 ± 0.15	0.11 ± 0.01	2.42 ± 0.15	2.46	0.98 ± 0.06	5.35 ± 0.08
1500	2.79 ± 0.16	0.08 ± 0.00	2.87 ± 0.16	2.45	1.17 ± 0.07	1.88 ± 0.06
2500	2.44 ± 0.17	0.07 ± 0.00	2.51 ± 0.17	2.47	1.02 ± 0.07	2.12 ± 0.12
3500	2.12 ± 0.16	0.09 ± 0.01	2.21 ± 0.16	2.47	0.90 ± 0.07	
St8/4 (#OPA324, 42.91°S, 63.08°E, 4998 m) <sup>d</sup>						
10	1.38 ± 0.14	0.80 ± 0.02	2.18 ± 0.14	2.52	0.87 ± 0.06	
46	1.19 ± 0.15	0.73 ± 0.02	1.92 ± 0.15	2.52	0.76 ± 0.06	
100	1.92 ± 0.15	0.33 ± 0.01	2.26 ± 0.15	2.52	0.90 ± 0.06	29.84 ± 0.19
200	2.21 ± 0.15	0.15 ± 0.01	2.36 ± 0.15	2.51	0.94 ± 0.06	21.81 ± 0.13
500	2.33 ± 0.16	0.08 ± 0.00	2.40 ± 0.16	2.50	0.96 ± 0.06	5.84 ± 0.09
1000	—	—	—	—	—	28.86 ± 0.51
1500	2.79 ± 0.17	0.10 ± 0.00	2.89 ± 0.17	2.44	1.18 ± 0.07	11.40 ± 0.10
2500	2.54 ± 0.16	0.08 ± 0.00	2.62 ± 0.16	2.47	1.06 ± 0.06	2.51 ± 0.06
3500	2.38 ± 0.16	0.09 ± 0.00	2.47 ± 0.16	2.47	1.00 ± 0.07	

<sup>a</sup>The station 3 was located in the Polar Front Zone during 4 days and  $^{234}\text{Th}$  activities were measured the first and the fourth day (3/1 and 3/4, respectively).

<sup>b</sup>The stations G1, G2 and G4 were located along the TOWYO transect during 4 h.

<sup>c</sup>The station 7 was located within the Subantarctic Front and the Subtropical Front during 5 days and  $^{234}\text{Th}$  activities were measured the second and the fifth day (7/2 and 7/5, respectively).

<sup>d</sup>The station 8 was located in the north the Agulhas Return Current during 4 days and  $^{234}\text{Th}$  activities were measured the last day (8/4).

with  $^{238}\text{U}$  concentrations (Coale and Bruland, 1985, 1987). Observing this equilibrium provides a test for the quality of the data. The beta counting results show that  $^{234}\text{Th}/^{238}\text{U}$  reached the equilibrium below the surface waters except at station 3/4 where values, after reaching equilibrium around 200–500 m, dropped down to 0.7 between 1500 and 3500 m. Such features were observed previously and several scenarios could explain the  $^{234}\text{Th}$  deficiency (Bacon et al., 1996; Benitez-Nelson et al., 2001).

Boundary scavenging or bottom sediments resuspension can induce a  $^{234}\text{Th}$  disequilibrium in the deep water column (Baskaran et al., 1996). However, the seafloor depth was 4300 m at station 3 and it is unlikely that an upwelling of bottom water was responsible for a such decrease of dissolved  $^{234}\text{Th}$ . Furthermore, we did not observe an increase of particulate  $^{234}\text{Th}$  that should be visible if there was a boundary scavenging or a resuspension of sediments.

Contributions from advection of a water mass with a deficit in dissolved  $^{234}\text{Th}$  could also explain the  $^{234}\text{Th}/^{238}\text{U}$  disequilibrium. At station 3, the vertical profile of  $^{230}\text{Th}$  concentrations was ex-

plained by the renewal of deep water by lateral transport of NADW from the Atlantic sector to the Indian sector on a time scale of 4–10 years (Coppola et al., 2003). This is far too slow to explain the  $^{234}\text{Th}/^{238}\text{U}$  disequilibrium. Similarly, from the potential temperature versus salinity data at station 3, the subduction of the Antarctic Intermediate Water (AAIW) was observed at 200 m and it cannot explain the  $^{234}\text{Th}/^{238}\text{U}$  disequilibrium at deeper depth (1500–3500 m).

Formation of the biological particles in the mesopelagic zone could explain the  $^{234}\text{Th}/^{238}\text{U}$  disequilibrium. In the study area, copepods always dominated in number and biomass with a maximum in the PFZ (Labat et al., 2002; Mayzaud et al., 2002). Strong variation of this grazing over distance and depth scales were observed at station 3 from the surface to 150 m (Mayzaud et al., 2002). Drifting sediment traps deployed at 200 m at station 3 collected a large amount of aggregates and some pteropods were observed inside the trap (Le Fèvre, unpublished data). This suggests that zooplankton could be responsible of aggregation of suspended particles settling below the surface

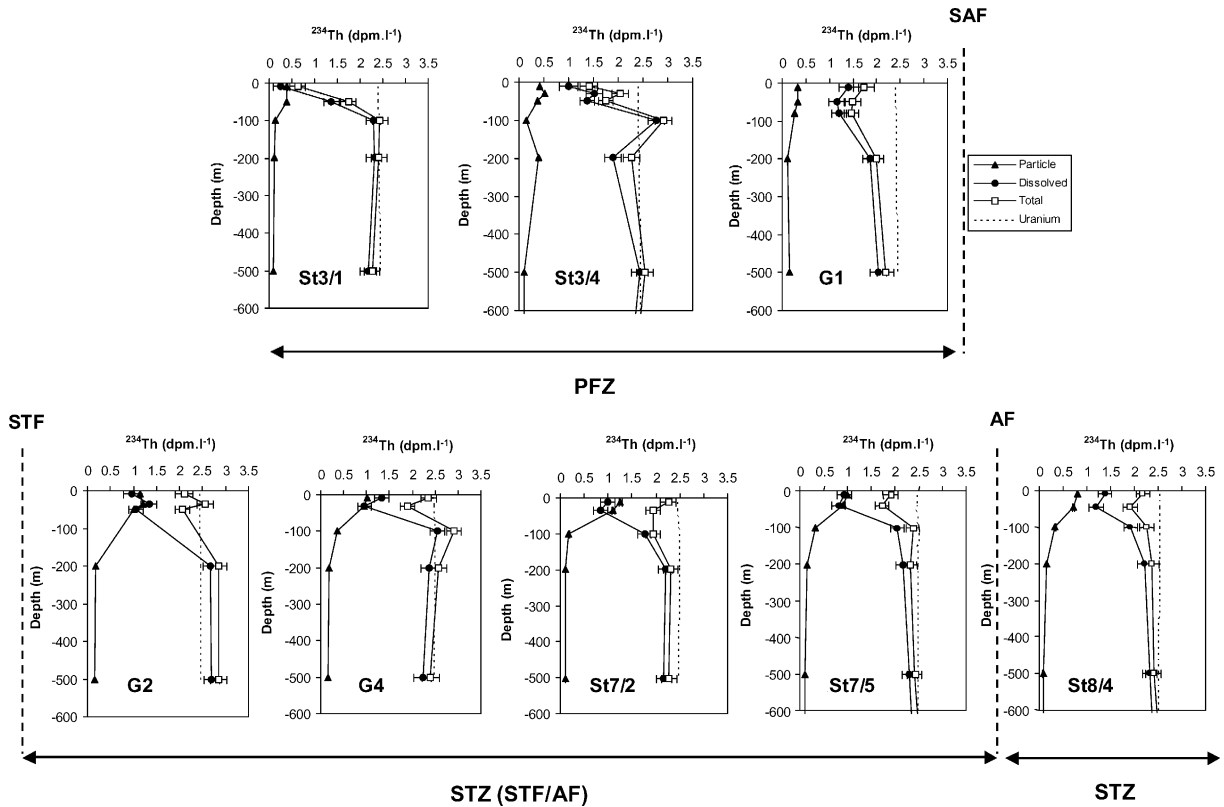


Fig. 2. Vertical profiles of  $^{234}\text{Th}$  activities between 0 and 500 m in the different zones studied during ANTARES 4 (PFZ = Polar Front Zone; SAF = Subantarctic Front; STF = Subtropical Front Zone; STZ = Subtropical Zone; AF = Agulhas Return Current).

layer. Although zooplankton data were not available at 1500 m depth and below, this mechanism taking place at 200 m, could induce a  $^{234}\text{Th}$  disequilibrium at deeper layer.

This last hypothesis seems to be the best explanation although the lack of information of the biogeochemical process in the mesopelagic zone constrains us to not exclude the possibility of analytical problems for deep samples at station 4.

#### 4.2. Calculation of $^{234}\text{Th}$ fluxes

To estimate the particulate  $^{234}\text{Th}$  flux exported from the surface water, we used the steady state (SS) scavenging model proposed by Coale and Bruland (1985). If we neglect the advective and diffusive transports, the  $^{234}\text{Th}$  export flux ( $P_{\text{Th}}^{\text{SS}}$ ) is defined by:

$$P_{\text{Th}}^{\text{SS}} = (A_{\text{U}} - A_{\text{Th}}) \times \lambda, \quad (1)$$

where  $A_{\text{U}}$  is the  $^{238}\text{U}$  activity,  $A_{\text{Th}}$  is the total  $^{234}\text{Th}$  activity and  $\lambda$  is the radioactive decay constant of  $^{234}\text{Th}$  ( $0.0288 \text{ d}^{-1}$ ). The term  $P_{\text{Th}}^{\text{SS}}$  is integrated to the depth where the  $^{234}\text{Th}/^{238}\text{U}$  equilibrium is reached (100 m).

The  $^{234}\text{Th}$  fluxes calculated at 100 m (below the mixed layer) for each station using the SS model are listed in Table 2. In the PFZ and the STZ,  $P_{\text{Th}}^{\text{SS}}$  ranged, respectively, from 735 to  $1831 \text{ dpm m}^{-2} \text{ day}^{-1}$  and from 311 to  $1254 \text{ dpm m}^{-2} \text{ d}^{-1}$ . These values are comparable to the  $^{234}\text{Th}$  export flux of  $865 \text{ dpm m}^{-2} \text{ d}^{-1}$  observed by Rutgers van der Loeff et al. (2002) in the Antarctic Polar Front region during the austral summer of 1996. For comparison, a  $^{234}\text{Th}$  export of  $3200 \text{ dpm m}^{-2} \text{ d}^{-1}$  was estimated during the spring bloom 1992 in the north of the Weddell Sea (Rutgers van der Loeff et al., 1997). In the Pacific sector of the Southern Ocean (along

Table 2  
Average of  $^{234}\text{Th}$  and POC fluxes and POC/ $^{234}\text{Th}$  ratios at 100 m depth.

Station	3/1	3/4	G1	G2	G4	7/2	7/5	8/4
Latitude south	46°	45.7°	45.2°	44.8°	44.3°	44°	44°	42.9°
Depth interval (m)	0–100	0–100	0–100	0–100	0–100	0–100	0–100	0–100
$^{234}\text{Th}$ flux (dpm m <sup>-2</sup> d <sup>-1</sup> )								
Steady-state model	1831 ± 95	735 ± 28	1627 ± 103	122 ± 6	311 ± 13	1212 ± 52	1254 ± 52	1187 ± 46
Non-steady state model	(–6009 ± 211) <sup>†</sup>				(1579 ± 247)			
POC/ $^{234}\text{Th}$ (μmol dpm <sup>-1</sup> )								
Small particles <sup>a</sup> (>0.6 μm)	20.9 ± 0.7	36.5 ± 1.4	14.7 ± 0.8	3.5 ± 0.2	8.3 ± 0.4	15.3 ± 0.6	11.9 ± 0.3	7.6 ± 0.2
Large particles <sup>b</sup> (>60 μm)	1.38 ± 0.02				0.79 ± 0.01			
POC flux <sup>c</sup> (mmolC m <sup>-2</sup> d <sup>-1</sup> )								
Steady-state model	2.53 ± 0.14	1.01 ± 0.04	2.25 ± 0.14	0.10 ± 0.02	0.25 ± 0.02	0.96 ± 0.04	0.99 ± 0.04	0.94 ± 0.04
Non-steady state model	(–8.29 ± 0.29) <sup>†</sup>				1.25 ± 0.20			

Fluxes are calculated in steady state and non-steady state conditions. POC/ $^{234}\text{Th}$  ratios are measured on small and large particles.

<sup>†</sup>Meaningless negative flux (see text for discussion).

<sup>a</sup>The POC/ $^{234}\text{Th}$  ratios on small particles were estimated from the  $^{234}\text{Th}$  activities and POC concentrations measured at 100 m.

<sup>b</sup>The POC concentrations on large particles were estimated from an average of POC measured at 30 and 200 m.

<sup>c</sup>POC fluxes are calculated with POC/ $^{234}\text{Th}$  ratios measured on large particles collected with the in situ pumps.

170°W), the  $^{234}\text{Th}$  fluxes, estimated with the SS model, ranged from 1800 to 3500 dpm m<sup>-2</sup> d<sup>-1</sup> and were relatively high compared to other sites and seasons (Buesseler et al., 2001).

The SS model is valid when the export flux is constant over periods of days to weeks. When a high flux period occurs (bloom), a non-steady state approach (NSS) is more appropriate (Buesseler et al., 1992, 1998, 2001; Cochran et al., 2000).

To apply a NSS model, we need sufficient time series data. During the ANTARES 4 cruise, we used the NSS model at the stations 3 and 7 where two  $^{234}\text{Th}$  vertical profiles have been measured over some days. To calculate the NSS  $^{234}\text{Th}$  derived flux, we used the approach of Buesseler et al. (1992):

$$\begin{aligned} \partial A_{\text{Th}} / \partial t &= (A_{\text{Th}_1} - A_{\text{Th}_2}) / (t_2 - t_1) \\ &= (A_{\text{U}} - A_{\text{Th}}) \times \lambda - P_{\text{Th}}^{\text{NSS}}, \end{aligned} \quad (2)$$

where  $A_{\text{Th}_1}$  and  $A_{\text{Th}_2}$  are the total  $^{234}\text{Th}$  activities measured at the time  $t_1$  and  $t_2$  ( $t = t_2 - t_1$ ) and  $P_{\text{Th}}^{\text{NSS}}$  represents the vertical  $^{234}\text{Th}$  flux estimated from the NSS model. If we suppose that this term is constant, the exported flux of  $^{234}\text{Th}$  becomes:

$$\begin{aligned} P_{\text{Th}}^{\text{NSS}} &= [\lambda / (1 - e^{-\lambda t})] \times [A_{\text{U}}(1 - e^{-\lambda t}) \\ &+ A_{\text{Th}_1} e^{-\lambda t} - A_{\text{Th}_2}]. \end{aligned} \quad (3)$$

At station 7, the SS  $^{234}\text{Th}$  flux were relatively similar between both sampling dates (Table 2), so that, the NSS  $^{234}\text{Th}$  flux is consistent with the SS model results. At station 3, the total  $^{234}\text{Th}$  activity was higher and the  $^{234}\text{Th}$  export SS flux was lower the last day than the first day (Table 2). This strong increase of  $^{234}\text{Th}$  activity produces a negative NSS  $^{234}\text{Th}$  flux.

The negative value of the NSS  $^{234}\text{Th}$  flux calculated at the station 3 could be explained by an upwelling of deeper and  $^{234}\text{Th}$  rich water due to a strong storm occurred that deepened the mixed layer depth from 26 to 56 m between the two sampling dates (Fig. 3). This process is not quantified in the NSS model and thus invalidating the use of such model at this station. Such inconsistent NSS fluxes were also observed for  $^{234}\text{Th}$  (Benitez-Nelson et al., 2001; Schmidt et al., 2002) and for  $^{210}\text{Pb}$ ,  $^{210}\text{Po}$  (Friedrich and Rutgers van der Loeff, 2002) with similar interpretation.

Finally, it seems more appropriate and self consistent to use the SS  $^{234}\text{Th}$  model to estimate the POC export fluxes at all stations.

#### 4.3. POC flux derived from $^{234}\text{Th}$

From the model derived  $^{234}\text{Th}$  flux, we can estimate a POC export from the upper

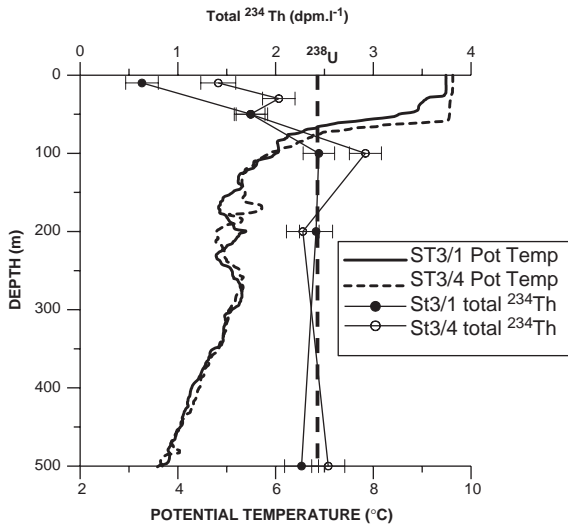


Fig. 3. Effect of the change of the mixed layer depth on the total  $^{234}\text{Th}$  vertical profiles between the stations 3/1 and 3/4.

100 m:

$$\text{POC flux} = (\text{POC}/^{234}\text{Th}) \times P_{\text{Th}}, \quad (4)$$

where  $P_{\text{Th}}$  is the SS  $^{234}\text{Th}$  flux as discussed in the previous section and  $\text{POC}/^{234}\text{Th}$  is the ratio measured on sinking particles. This equation is empirical and supposes that  $^{234}\text{Th}$  and POC are carried on the same particles below the euphotic zone (Buesseler, 1998). The  $^{234}\text{Th}$  method depends on the variability in the  $\text{POC}/^{234}\text{Th}$  ratio and  $^{234}\text{Th}$  flux. Moran et al. (2003) indicated that the natural variability in the  $\text{POC}/^{234}\text{Th}$  ratio, combined with different criteria used to estimate the depth-integrated  $^{234}\text{Th}$  flux, can result in 2–10 fold uncertainty in the POC export flux. The crucial point is to estimate the  $\text{POC}/^{234}\text{Th}$  ratio on the sinking particles and how can we measure accurately the sinking particles (Benitez-Nelson and Charette, 2004).

The tools used for the  $\text{POC}/^{234}\text{Th}$  estimations are crucial for the quality and the accuracy of the sinking fraction. The sediment trap may have hydrodynamic biases and also contamination from “swimmers”. The in situ pumps filtration collect both suspended and sinking particles that could be fractionated during the filtration of the sample. In the present study, the small and large particles have been collected with Niskin bottles and in situ

large volume pumps, respectively. Ideally, the sediment traps would be a better choice to measure the sinking particulate fraction but unfortunately the amount of material collected in the drifting traps were not sufficient for on board  $^{234}\text{Th}$  analysis.

To constrain the variability of the  $\text{POC}/^{234}\text{Th}$  ratio, we measured POC and  $^{234}\text{Th}$  on small ( $>0.6\ \mu\text{m}$ ) and large ( $>60\ \mu\text{m}$ ) particles. In the present study, we integrated the  $^{234}\text{Th}$  disequilibrium fluxes from 0 to 100 m using the trapezoidal method described by Buesseler et al. (1992) and we calculated the  $\text{POC}/^{234}\text{Th}$  ratio at the base of the depth interval (100 m). This method seems to be the key to minimize the uncertainties of the POC export flux from the  $^{234}\text{Th}/^{238}\text{U}$  disequilibrium technique (Benitez-Nelson and Charette, 2004). For the  $\text{POC}/^{234}\text{Th}$  assessment, we evaluated this ratio on small and large particles. The POC concentrations on small particles were measured by Leblanc et al. (2002) at 100 m whereas POC concentrations on large particles were analyzed by Panagiotopoulos et al. (2002) at 30 and 200 m for only two stations (3 and 7). To be consistent with the  $^{234}\text{Th}$  activities measured on large particles at 100 m at both stations (3 and 7) and with the  $^{234}\text{Th}/^{238}\text{U}$  disequilibrium profiles, we evaluated the POC concentrations on large particles at 100 m by averaging the values of POC measured at 30 and 200 m.

For the small particles, the  $\text{POC}/^{234}\text{Th}$  ratio at 100 m ranged from 3.5 to 36.5  $\mu\text{mol dpm}^{-1}$ . For the large particles collected with in situ pumps, the  $\text{POC}/^{234}\text{Th}$  ratio at 100 m is lower and is estimated to 1.38 and 0.79  $\mu\text{mol dpm}^{-1}$  at stations 3 (PFZ) and 7 (STZ), respectively (Table 2). As suggested in previous studies, the  $\text{POC}/^{234}\text{Th}$  ratio decreases when the particle size increases as a result of carbon respiration by grazers and/or microbial degradation in the process of particle aggregation (Andersson et al., 2000; Buesseler et al., 1995; Burd et al., 2000; Coppola et al., 2002; Moran et al., 1993). Concerning this study, two explanations can account for the difference of the  $\text{POC}/^{234}\text{Th}$  ratios in large and small particles: the low POC concentration in the large particles due to remineralization and/or the large presence in the small particles of old detrital organic matter that has lost

its  $^{234}\text{Th}$ . The presence of detrital POC is supported by the high POC/Chl *a* found in the particulate matter (Leblanc et al., 2002). These characteristics are associated with the end of bloom conditions observed during the ANTARES 4 cruise. Indeed, the surface distribution of Chl *a* from SeaWiFS composite imagery for the cruise period showed higher values in December 1998 ( $1\text{--}2\text{ mg m}^{-3}$ ) and decreasing in January–February 1999 ( $0.3\text{--}0.5\text{ mg m}^{-3}$ ; Le Fèvre, 2000). This is confirmed by the data collected during ANTARES 4: (1) at all stations, the biogenic silica (BSi) and POC productions were very low, due to limitation of nutrient availability; (2) the poor preservation state of diatom frustules of *Pseudonitzschia* spp. suggested by the BSi/POC ratio of the particulate matter indicating that the phytoplankton had shifted towards a nanoplanktonic community dominated by flagellates and typical of the end of bloom period (Leblanc et al., 2002).

The POC/ $^{234}\text{Th}$  ratios on small and large particles are higher in the PFZ than in the STZ (Table 2). In the STZ, Leblanc et al. (2002) noted the presence of diatoms at the end of the productive stage. Diatom frustules are poor in

carbon but yield ample surface area for  $^{234}\text{Th}$  adsorption, which could produce a low POC/ $^{234}\text{Th}$  ratios (Rutgers van der Loeff et al., 1997). During the ANTARES 4, the POC consumption rate ( $k_{\text{POC}}$ ) by bacteria in large particles was determined through incubation experiments (Panagiotopoulos et al., 2002). Values ranged from  $0.012\text{ d}^{-1}$  for the station 3 to  $0.031\text{ d}^{-1}$  for the station 7. It is slower or equal to the radioactive decay of  $^{234}\text{Th}$  ( $\lambda_{^{234}\text{Th}} = 0.028\text{ d}^{-1}$ ) suggesting that bacterial remineralization of the large particles cannot account for their low POC/ $^{234}\text{Th}$  ratio.

To estimate the POC fluxes, the POC/ $^{234}\text{Th}$  ratios on large filtered particles are the most appropriate to represent the sinking particulate fraction. Assuming that the POC/ $^{234}\text{Th}$  ratios estimated at stations 3 and 7 are, respectively, representative to the sampling zone PFZ and STZ, the POC fluxes calculated with the SS  $^{234}\text{Th}$  model at 100 m range from  $0.10$  to  $2.53\text{ mmol C m}^{-2}\text{ d}^{-1}$  (Table 2 and Fig. 4). They are higher in the PFZ (average of  $1.93\text{ mmol C m}^{-2}\text{ d}^{-1}$ ) than in the STZ (average of  $0.65\text{ mmol C m}^{-2}\text{ d}^{-1}$ ). These POC fluxes derived from the  $^{234}\text{Th}$  method are relatively higher to those measured directly with drifting

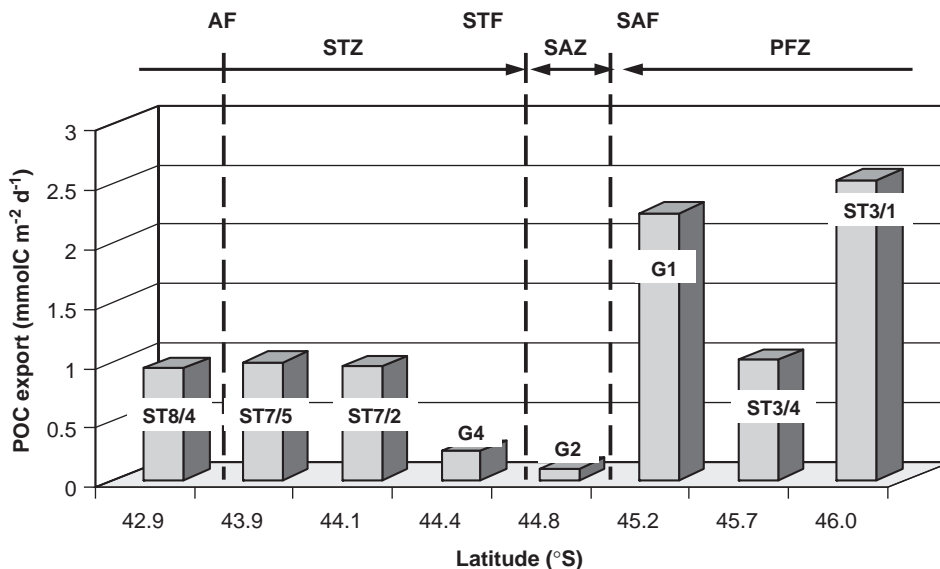


Fig. 4. POC fluxes ( $\text{mmol C m}^{-2}\text{ d}^{-1}$ ) at 100 m vs. latitude derived from  $^{234}\text{Th}$  data in steady state model. The dashed line represents the position of fronts in the ANTARES 4 zone (SAF: Subantarctic Front; STF: Subtropical Front; AF: Agulhas return current).

traps deployed at 200 m at stations 3 and 8 ( $1.26$  and  $0.42 \text{ mmolC m}^{-2} \text{ d}^{-1}$ , respectively) reflecting a preferential remineralization of carbon. However, at station 8, the  $^{234}\text{Th}$  activity of large particles was measured at 200 m so it was possible to estimate the POC flux ( $0.35 \pm 0.01 \text{ mmolC m}^{-2} \text{ d}^{-1}$ ) at the same depth than the sediment trap. The agreement between this estimate and the POC flux collected by the trap at 200 m suggests that the assumptions established in the  $^{234}\text{Th}$  model (steady state and  $\text{POC}/^{234}\text{Th}$  ratio on large particles) are suitable to estimate an accurate POC export at station 8 and we can suppose that this conclusion is also applicable for all sampling area.

Panagiotopoulos et al. (2002) have also evaluated the POC export from the POC concentrations collected on the in situ pump filters ( $> 60 \mu\text{m}$ ) and assuming a settling velocity of  $100 \text{ m d}^{-1}$ . They estimated a POC sinking flux at 200 m of  $0.57 \text{ mmolC m}^{-2} \text{ d}^{-1}$  and  $0.43 \text{ mmolC m}^{-2} \text{ d}^{-1}$  at stations 3 and 7, respectively. Although their calculations are in agreement with our results at station 7 (Table 2), the POC export that we estimated at station 3 is higher. This probably reflects that the settling velocity varies with the type of particles and the biogeochemical conditions of the zone and cannot be considered always equal to  $100 \text{ m d}^{-1}$ .

During ANTARES 4, Cattaldo et al. (2000) studied the suspended biogenic barium (assimilated to barite) in the water column as a proxy of exported organic carbon (Dehairs et al., 1997, 2000). From the barium (Ba) concentrations on suspended particles collected in mesopelagic waters (between 100 and 500 m), they estimated a POC export from 2 to  $8 \text{ mmolC m}^{-2} \text{ d}^{-1}$  (Dehairs et al., 2000). These values are 50–160% higher than those calculated from  $^{234}\text{Th}$ . Following Dehairs et al. (1997), the suspended barite maximum is directly related to the mineralization of organic matter exported from the surface layers at these depths. Consequently, the POC export fluxes estimated from Ba correspond to consumed carbon fluxes (respired) in the mesopelagic zone. If the carbon fluxes, deduced from  $^{234}\text{Th}$  and Ba, were equal, this would suggest that all POC is remineralized during the export to the deep waters

(Jeandel et al., 2000). The large difference observed between both estimates of the POC fluxes, in this study, may reflect the different time scales recorded by  $^{234}\text{Th}$  and Ba. The POC export flux estimated from  $^{234}\text{Th}$  is on time scale of one month. In contrast, the POC fluxes estimated from particulate Ba in the water column are integrated over a longer period that includes the high export spring bloom.

#### 4.4. POC export variability in the Southern Ocean

Comparison between POC export fluxes estimated in the Southern Ocean is difficult because the Southern Ocean is made of sectors characterized by different biogeochemical regimes and different tools (sediment traps, in situ pumps, bottles) were used in previous studies to estimate the POC export fluxes (Buesseler et al., 2001; Cochran et al., 2000; Rutgers van der Loeff et al., 1997, 2002; Trull et al., 2001). Nevertheless, the discussion remains important to show the seasonal variations of the POC export and the relative importance of the positions of the fronts (SAF, STF and AF) in the carbon export evaluation. The POC export fluxes estimated during the ANTARES 4 cruise are lower than those calculated from  $^{234}\text{Th}$  in the previous studies located in the Southern Ocean (Table 3). This difference is mainly due to the low  $\text{POC}/^{234}\text{Th}$  ratios observed during ANTARES 4 rather than to the extent of  $^{238}\text{U}$ – $^{234}\text{Th}$  disequilibrium. Others natural processes could also change the POC export as the preferential recycling of POC, the plankton species and the grazing effects of zooplankton. In the STZ, where the POC export flux is lower, the sea surface temperature appeared high enough to allow a high recycling of BSi (Leblanc et al., 2002) and could also induce higher organic matter degradation.

In the Pacific sector, very high POC export were observed in the Ross Sea gyre and in the AESOPS project zone (transect along  $170^\circ\text{W}$  and  $55$ – $72^\circ\text{S}$ ) where a pronounced ice edge ablation/retreat occurs in addition to a predominance of large diatoms and consequently these results are not really comparable to our study (Buesseler et al., 2001; Cochran et al., 2000). However, in the

Table 3

POC export ( $\text{mmolC m}^{-2} \text{d}^{-1}$ ) calculated from the  $^{234}\text{Th}/^{238}\text{U}$  disequilibrium at steady state and  $\text{POC}/^{234}\text{Th}$  ratio at 100 m depth in different region of the Southern Ocean

Location	Date	$^{234}\text{Th}$ flux ( $\text{dpm m}^{-2} \text{d}^{-1}$ )	$\text{POC}/^{234}\text{Th}$ ( $\mu\text{mol dpm}^{-1}$ )	POC flux ( $\text{mmolC m}^{-2} \text{d}^{-1}$ )	Reference
Atlantic sector:ANT X/6	November–October 1992	3200	20.9 <sup>a</sup>	20–40 <sup>c</sup>	Rutgers van der Loeff et al., 1997
Atlantic sector:ANT XIII/2	December–January 1996	865	10.15 <sup>a</sup>	8.8 <sup>c</sup>	Rutgers van der Loeff et al., 2002
Ross Sea	October 96/January 1997–February/April 1997	200–2600	2.5–3.5 <sup>b</sup>	7–91	Cochran et al., 2000
Pacific sector:AESOPS	October 96/January 1997–February/April 1997	1800–3600	3–6.6 <sup>b</sup>	10–15	Buesseler et al., 2001
Australian sector:SAZ	September 1997–February 1998	—	—	0.1–0.3 <sup>d</sup>	Trull et al., 2001
Indian sector	January–February 1999	120–1800	0.8–1.4 <sup>b</sup>	0.1–2.5	This study

<sup>a</sup> $\text{POC}/^{234}\text{Th}$  ratios were measured on small particles ( $> 1 \mu\text{m}$ )

<sup>b</sup> $\text{POC}/^{234}\text{Th}$  ratios were calculated by filtration of large particles ( $> 60\text{--}70 \mu\text{m}$ )

<sup>c</sup>The POC fluxes observed were estimated assuming that the  $\text{POC}/^{234}\text{Th}$  ratio on exported particles is 30–60% of that measured on suspended particles.

<sup>d</sup>The values were collected from moored sediment traps deployed from 1060 to 3850 m.

northern part of the AESOPS section (north of the PFZ and in the SAZ), variable POC export were observed ( $5\text{--}15 \text{mmolC m}^{-2} \text{d}^{-1}$ ) even in the summer period. These POC fluxes were explained by the presence of fecal pellets and marine snow in the water column. In the opposite, the  $^{234}\text{Th}$  activities measured during the mesoscale iron fertilization experiment (SOIREE) in the Pacific sector revealed no increase of the POC export (Charette and Buesseler, 2000; Nodder and Waite, 2001). The reasons evoked were the cold seawater temperatures that slowed down phytoplankton activity and particle aggregation or the limited period of observation that might have been shorter than the production-export sequence (Boyd et al., 2000; Charette and Buesseler, 2000).

In the Atlantic sector, the spring situation was studied (Rutgers van der Loeff et al., 2002). As in the AESOPS study, the POC export was around  $10 \text{mmolC m}^{-2} \text{d}^{-1}$  in the north of the PFZ and in the SAZ. However, this estimate must be taken with caution because it was based on the high  $\text{POC}/^{234}\text{Th}$  ratios of the small particle fraction (large particles were not analyzed) and therefore we consider it rather as an upper limit.

Finally, the Australian sector (south of Tasmania  $\sim 140\text{--}141^\circ\text{E}$ ) seems to be the most comparable

to the Indian sector because the fronts are similar and widely separated between  $\sim 40\text{--}50^\circ\text{S}$  and the phytoplankton community was predominated by nano- and pico-size flagellates as in ANTARES 4 (Kopczynska et al., 2001). In this sector, the SAZ (Subantarctic Zone) campaign used sediment traps moorings to estimate the POC export from September 1997 to February 1998 (Trull et al., 2001). The POC flux collected at 1060 m depth at station located around  $47^\circ\text{S}$  and  $142^\circ\text{E}$  from January to February 1998 ranged from 0.31 to  $1.42 \text{mmolC m}^{-2} \text{d}^{-1}$ . These POC values measured independently from  $^{234}\text{Th}$  are similar to those observed during ANTARES 4 at the same period of the year. However, that comparison of the SAZ traps with the ANTARES 4 traps should be made with caution because the trapping efficiency during the SAZ campaign was about 60% (Trull et al., 2001) and because remineralization between 100 and 1000 m may substantially reduce the SAZ POC fluxes (Martin et al., 1987).

#### 4.5. Export, primary production and biogeochemical implications

In the HNLC Southern Ocean, the phytoplankton community and the primary production are

controlled by the availability of three resources (light, iron and silicic acid), the grazing pressure and low water temperatures which vary seasonally (De Baar and Boyd, 2000; Rintoul and Trull, 2001). During ANTARES 4, the chlorophyll levels were low ( $<0.7 \text{ mg/m}^3$ ) and the primary production was limited by iron and co-limited by silica for siliceous species in the PFZ and the SAZ. In the STZ, the limitation was primarily due to nitrate but levels of iron and dissolved silica were also low (Sedwick et al., 2002; Blain et al., 2002).

The relationship between primary production and carbon export is complex. To compare both processes, Buesseler (1998) defined the ThE as ratio between the carbon export estimated from the  $^{234}\text{Th}$  activities and the primary production. The export ratio ThE is commonly  $<5\text{--}10\%$  in open ocean but higher values were associated with seasonal diatom blooms in the Arabian Sea (30–50%; Buesseler, 1998) and in the Pacific sector of the Southern Ocean (15–25% in the Subantarctic zones along  $170^\circ\text{W}$ ; Buesseler et al., 2001).

During ANTARES 4, the ThE ratio represents only 1–7%. Nevertheless, we have to note that the primary production was estimated by incorporation of  $^{14}\text{C}$  labeled substrate and consequently integrated over the time of the  $^{14}\text{C}$  incubation (12–24 h) whereas  $^{234}\text{Th}$  averages over periods of weeks. This suggests the possibility that the ThE ratio is biased by these different time scales as much as 1–2 months may occur between the maximum primary production and the maximum export production (Buesseler, 1998). As noted earlier, ANTARES 4 occurred around one month after the bloom. Therefore, we may strongly overestimate the ThE ratio if we compare the export of the POC produced during the bloom with the nutrient-limited primary production prevailing during the cruise. In addition,  $^{234}\text{Th}$  disequilibrium integrates  $^{234}\text{Th}$  export over 35 days so that, at the end of the bloom, comparison of the POC export derived from  $^{234}\text{Th}$  with the actual primary production also tends to overestimate the ThE ratio when the particulate flux decreases with time. The extent these 2 bias is not clear a priori but as the  $^{234}\text{Th}$  export is at steady

state (station 7) and as there is a good agreement between the  $^{234}\text{Th}$ -derived POC fluxes and the drifting trap measurement at station 3 (also suggesting steady state), we expect the POC export to be at steady state and that it can be compared to the estimated primary production.

It remains that the low ThE ratio at ANTARES 4 represents an upper limit of the export ratio and suggests a high carbon remineralization process (Buesseler et al., 2001). This idea agrees with the lower average annual water column preservation efficiency (ratio between the annual POC export at 1000 m and annual primary production) in the Indian sector compared to the Pacific and Atlantic sectors of the Southern Ocean (Pilskaal et al., 2003). During ANTARES 4, Leblanc et al. (2002) measured a primary production integrated over 150 m. Value was higher at station 7 ( $44.2 \text{ mmolCm}^{-2} \text{ d}^{-1}$ ) than at station 3 ( $27.6 \text{ mmolCm}^{-2} \text{ d}^{-1}$ ). The export  $^{234}\text{Th}$  derived POC was maximum at station 3. This indicates that the carbon export and the primary production had opposite variation due to the time delay induced by both estimations and/or due to zonal variability of the remineralization process. The time delay between the development of the bloom and the carbon export is still a crucial question that has to be clarified.

In the Southern Ocean, the low grazing pressure and the efficient vertical transport of diatoms lead to relatively high export ratios even during the lowest productivity periods (Buesseler et al., 2001). In the present study, however, different parameters could contribute to a low export ratio:

- (1) The low grazing rates exerted by mesozooplankton on the phytoplankton primary production inducing a limited export of POC (Mayzaud et al., 2002)
- (2) The predominance of micro- and nano-size flagellates, typical at the end of the bloom, could reduce the POC export (Leblanc et al., 2002)
- (3) The zonal variability of POC export is explained by the sea surface temperature in the STZ which appeared high enough to allow a fast BSi recycling and a high organic matter degradation rate (Leblanc et al., 2002)

(4) In addition to that, the mineralization of labile organic carbon by an efficient microbial loop observed in the STZ could explain the low POC export to the deep layers (Panagiotopoulos et al., 2002). The respiratory activity estimated by electron transport system (ETS) in microbial communities indicates a higher water column remineralization in the STZ compare to the PFZ and it is consistent with the zonal variability of the POC flux (Aristegui et al., 2002).

## 5. Conclusion

The use of  $^{234}\text{Th}$  allowed the characterization of the spatial patterns in POC export fluxes in the Indian sector of the Southern Ocean. In summer, the frontal zone of the Indian sector was characterized by a low export production. This could be explained by a decoupling between primary and export production due probably to a low grazing effect or by a low predominance of diatoms typical at the end of the bloom. In addition, we observed that the POC fluxes were lower in the STZ than in the PFZ. These results were in agreement with independent biogeochemical observations during ANTARES 4. A strong remineralization process and/or a high bacterial activity could explain the low proportion of sinking POC leaving the euphotic zone in the STZ (Leblanc et al., 2002; Panagiotopoulos et al., 2002). This demonstrates the strong zonal variability existing in the Southern Ocean in terms of POC export and the difficulty to use one sector as biogeochemical model for such large and dynamic system. It has been suggested that an increase on the export production in the Southern Ocean, in response to the iron inputs, could decrease the atmospheric  $\text{CO}_2$  level (Boyd et al., 2000; Martin et al., 1991, 1994). However, the previous iron fertilization experiments (SOIREE, EISENEX) did not resolve the question about the carbon export below the mixed layer (Boyd, 2002; Charette and Buesseler, 2000). There is a lack of knowledge concerning the remineralization and recycling processes of organic matter in intermediate-deep waters. This would be a high priority for the future programs.

## Acknowledgements

We thank captain and crew of Marion Dufresne for their assistance during expedition ANTARES 4. We thank M. Denis for his effort in organizing ANTARES 4. M. Rutgers van der Loeff is warmly thanked for sharing his experience of the  $^{234}\text{Th}$  measurement with us. We thank also R. Sempéré, C. Panagiotopoulos, T. Cattaldo, B. Queguiner and K. Leblanc for their help to provide information about the carbon concentrations, large particle sampling and carbon fluxes in the sediment traps. We would like also express gratitude to C. Bournot for her help in using the large volume pumps during the cruise. IAEA-MEL operates under a bilateral agreement between the IAEA and the Government of the Principality of Monaco. We thank M. Bacon and 3 anonymous reviewers for their very constructive comments.

## References

- Andersson, P.S., Gustafsson, Ö., Roos, P., Broman, D., Toneyby, A., 2000. Particle mediated surface water export: Comparison of estimates from  $^{238}\text{U}$ – $^{234}\text{Th}$  disequilibria and sediment traps in a continental shelf region, AGU Ocean Science Meeting, San Antonio, TX.
- Aristegui, J., Denis, M., Almunia, J., Montero, M.F., 2002. Water-column remineralization in the Indian sector of the Southern Ocean during early spring. *Deep Sea Research II* 49, 1707–1720.
- Bacon, M.P., Cochran, J.K., Hirschberg, D., Hammar, T.R., Fleer, A.P., 1996. Export flux of carbon at the equator during EqPac time-series cruises estimated from  $^{234}\text{Th}$  measurements. *Deep Sea Research II* 43, 1133–1153.
- Baskaran, M., Santschi, P.H., Guo, L., Bianchi, T.S., Lambert, C., 1996.  $^{234}\text{Th}$ : $^{238}\text{U}$  disequilibria in the Gulf of Mexico: the importance of organic matter and particle concentration. *Continental Shelf Research* 16 (3), 353–380.
- Baskaran, M., Swarzenski, P.W., Porcelli, D., 2003. Role of colloidal material in the removal of  $^{234}\text{Th}$  in the Canada basin of the Arctic Ocean. *Deep Sea Research I* 50, 1353–1373.
- Benitez-Nelson, C.R., Charette, M.A., 2004. Uncertainty versus variability in upper ocean carbon flux estimates. *Limnology and Oceanography* 49 (4), 1218–1220.
- Benitez-Nelson, C.R., Buesseler, K.O., Karl, D.M., Andrews, J.E., 2001. A time-series study of particulate matter export in the North Pacific Subtropical Gyre based on  $^{234}\text{Th}$ :  $^{238}\text{U}$  disequilibrium. *Deep-Sea Research I* 48, 2595–2611.
- Blain, S., Sedwick, P.N., Griffiths, F.B., Quéguiner, B., Bucciarelli, E., Fiala, M., Pondaven, P., Tréguer, P., 2002.

- Quantification of algal iron requirements in the Subantarctic Southern Ocean (Indian sector). *Deep Sea Research II* 49, 3255–3273.
- Boyd, P.W., 2002. The role of iron in the biogeochemistry of the Southern Ocean and equatorial Pacific: a comparison of in situ iron enrichments. *Deep Sea Research Part II: Topical Studies in Oceanography* 49 (9–10), 1803–1821.
- Boyd, P.W., Watson, A.J., Law, C.S., Abraham, E.R., Trull, T., Murdoch, R., Bakker, D.C.E., Bowie, A., Buesseler, K.O., Chang, H., Charette, M., Croot, P., Downing, K., Frew, R., Gall, M., Hadfield, M., Hall, J., Harvey, M., Jameson, G., LaRoche, J., Liddicoat, M., Ling, R., Maldonado, M.T., McKay, R.M., Nodder, S., Pickmere, S., Pridmore, R., Rintoul, S., Safi, K., Sutton, P., Strzepek, R., Tanneberger, K., Turner, S., Waite, A., Zeldis, J., 2000. A mesoscale phytoplankton bloom in the polar Southern Ocean stimulated by iron fertilization. *Nature* 407, 695–702.
- Buesseler, K.O., 1998. The decoupling of production and particulate export in the surface ocean. *Global Biogeochemical Cycles* 12 (2), 297–310.
- Buesseler, K.O., Bacon, M., Cochran, J.K., Livingston, H.D., 1992. Carbon and nitrogen export during the JGOFS North Atlantic Bloom Experiment estimated from  $^{234}\text{Th}$ : $^{238}\text{U}$  disequilibria. *Deep Sea Research* 39, 1115–1137.
- Buesseler, K.O., Andrews, J.A., Hartman, M.C., Belostock, R., Chai, F., 1995. Regional estimates of the export flux of particulate organic carbon derived from thorium- $^{234}$  during the JGOFS EQPAC Program. *Deep Sea Research II* 42 (2–3), 777–804.
- Buesseler, K.O., Ball, L., Andrews, J., Benitez-Nelson, C., Belostock, R., Chai, F., Chao, Y., 1998. Upper ocean export of particulate organic carbon in the Arabian Sea derived from thorium- $^{234}$ . *Deep Sea Research* 45, 2461–2487.
- Buesseler, K.O., Ball, L., Andrews, J., Cochran, J.K., Hirschberg, D.J., Bacon, M.P., Fleer, A., Brzezinski, M., 2001. Upper ocean export of particulate organic carbon and biogenic silica in the Southern Ocean along 170°W. *Deep Sea Research II* 48, 4275–4297.
- Burd, A.B., Moran, S.B., Jackson, G.A., 2000. A coupled adsorption-aggregation model of the POC/ $^{234}\text{Th}$  ratio of marine particles. *Deep Sea Research Part I* 47, 103–120.
- Cattaldo, T., Dehairs, F., Cardinal, D., Navez, J., 2000. Ba and Sr uptake by phytoplankton and suspended matter in SAZ and PFZ of the Australian and Indian sectors of the Southern Ocean, SO-JGOFS symposium, Brest, France.
- Charette, M.A., Buesseler, K.O., 2000. Delay in the onset of particle export during an iron fertilization experiment in the Southern Ocean. *Geochemistry, Geophysics, Geosystems* 1, paper number 2000GC000069.
- Chen, J.H., Edwards, R.L., Wasserburg, G.J., 1986.  $^{238}\text{U}$ – $^{234}\text{U}$  and  $^{232}\text{Th}$  in seawater. *Earth and Planetary Science Letters* 80, 241–251.
- Coale, K.H., Bruland, K.W., 1985.  $^{234}\text{Th}$ : $^{238}\text{U}$  disequilibria within the California current. *Limnology and Oceanography* 30, 22–33.
- Coale, K.H., Bruland, K.W., 1987. Oceanic stratified euphotic zone as elucidated by  $^{234}\text{Th}$ : $^{238}\text{U}$  disequilibria. *Limnology and Oceanography* 32, 189–200.
- Cochran, J.K., Buesseler, K.O., Bacon, M.P., Wang, H.W., Hirschberg, D.J., Ball, L., Andrews, J., Crossin, G., Fleer, A., 2000. Short-lived thorium isotopes ( $^{234}\text{Th}$ ,  $^{228}\text{Th}$ ) as indicators of POC export and particle cycling in the Ross Sea, Southern Ocean. *Deep-Sea Research II* 47 (15–16), 3451–3490.
- Coppola, L., Roy-Barman, M., Wassmann, P., Jeandel, C., 2002. Calibration of sediment traps and particulate organic carbon export using  $^{234}\text{Th}$  in the Barents Sea. *Marine Chemistry* 80 (1), 11–26.
- Coppola, L., Roy-Barman, M., Jeandel, C., Mulsow, S., Povinec, P., 2003. Study of  $^{234}\text{Th}$ ,  $^{232}\text{Th}$  and  $^{230}\text{Th}$  in the Indian sector of the Southern Ocean, EGS—AGU—EUG Joint Assembly, Nice, France.
- De Baar, H.J.W., Boyd, P.W., 2000. The Role of Iron in Plankton Ecology and Carbon Dioxide Transfer of the Global Oceans. In: Hanson, R.B., Ducklow, H.W., Field, J.G. (Eds.), *The Dynamic Ocean Carbon Cycle: A Midterm Synthesis of the Joint Global Ocean Flux Study*. International Geosphere Biosphere Programme Book Series, Vol. 5. Cambridge University Press, Cambridge, pp. 61–140 (Chapter 4).
- De Baar, H.J.W., de Jong, J.T.M., Bakker, D.C.E., Löscher, B.M., Veth, C., Bathman, U., Smetacek, V., 1995. Importance of iron for plankton blooms and carbon dioxide drawdown in the Southern Ocean. *Nature* 373, 412–415.
- Dehairs, F., Shopova, D., Ober, S., Veth, C., Goeyens, L., 1997. Particulate barium stocks and oxygen consumption in the Southern Ocean mesopleagic water column during spring and early summer: Relationship with export production. *Deep Sea Research II* 44, 497–516.
- Dehairs, F., Cattaldo, T., Cardinal, D., Kocczynska, E., Elskens, M., 2000. Export of organic matter from the subantarctic and the Polar Front zone: confronting the bottom-up Ba proxy and the top-down new production approaches, SO-JGOFS symposium, Brest, France.
- Friedrich, J., Rutgers van der Loeff, M.M., 2002. A two-tracer ( $^{210}\text{Po}$ – $^{234}\text{Th}$ ) approach to distinguish organic carbon and biogenic silica export flux in the Antarctic Circumpolar Current. *Deep Sea Research I* 49, 101–120.
- Jeandel, C., Tachikawa, K., Bory, A., Dehairs, F., 2000. Biogenic barium in suspended and trapped material as a tracer of export production in the tropical NE Atlantic (EUMELI sites). *Marine Chemistry* 71, 125–142.
- Kocczynska, E.E., Dehairs, F., Elskens, M., Wright, S., 2001. Phytoplankton and microzooplankton variability between the Subtropical and Polar Fronts south of Australia: Thriving under regenerative and new production in late summer. *Journal of Geophysical Research* 106 (C12), 31597–31609.
- Labat, J.P., Mayzaud, P., Dallot, S., Errhif, A., Razouls, S., Sabini, S., 2002. Mesoscale distribution of zooplankton in

- the Sub-Antarctic Frontal system in the Indian part of the Southern Ocean: a comparison between optical plankton counter and net sampling. *Deep Sea Research I* 49, 735–749.
- Le Fèvre, J., 2000. Mesoscale dynamics and phytoplankton biomass associated with a frontal system in the Southern Ocean: exploitation of SeaWIFS images received in near real time during cruise Antares 4, Southern Ocean JGOFS Symposium, Brest, France.
- Leblanc, K., Quéguiner, B., Fiala, M., Blain, S., Morvan, J., Corvaisier, R., 2002. Particulate biogenic silica and carbon production rates and particulate matter distribution in the Indian sector of the Subantarctic Ocean. *Deep Sea Research II* 49 (16), 3189–3206.
- Martin, J.H., Knauer, G.A., Karl, D., Broenkow, W.W., 1987. VERTEX: Carbon cycling in the northeast Pacific. *Deep Sea Research* 34, 267–285.
- Martin, J.H., Gordon, R.M., Fitzwater, S.E., 1991. The case for iron. *Limnology and Oceanography* 36 (8), 1793–1802.
- Martin, J.H., Coale, K.H., Johnson, K.S., Fitzwater, S.E., Gordon, R.M., Tanner, S.J., Hunter, C.N., Elrod, V.A., Nowiiki, J.L., Coley, T.L., Barber, R.T., Lindley, S., Watson, A.J., Scoy, K.V., Law, C.S., Liddicoat, M.I., Ling, R., Stanton, T., Stockel, J., Collins, C., Anderson, A., Bidigare, R., Ondrusek, M., Latasa, M., Millero, F.J., Lee, K., Yao, W., Zhang, J.Z., Friederich, G., Sakamoto, C., Chavez, F., Buck, K., Kolber, Z., Greene, R., Falkowski, P., Chisholm, S.W., Hoge, F., Swift, R., Yungel, J., Turner, S., Nightingale, P., Hatton, A., Liss, P., Tindale, N.W., 1994. Testing the iron hypothesis in ecosystems of the equatorial Pacific Ocean. *Nature* 371, 123–129.
- Mayzaud, P., Tirelli, V., Errhif, A., Labat, J.P., Razouls, S., Perissinotto, R., 2002. Carbon intake by zooplankton. Importance and role of zooplankton grazing in the Indian sector of the Southern Ocean. *Deep Sea Research II* 49, 3169–3187.
- Metzl, N., Tilbrook, B., Poisson, A., 1999. The annual fCO<sub>2</sub> cycle and the air-sea CO<sub>2</sub> flux in the sub-Antarctic Ocean. *Tellus Series B Chemical and Physical Meteorology* 51 (4), 849–861.
- Moran, S.B., Buesseler, K.O., Niven, S.E.H., Bacon, M.P., Cochran, J.K., Livingston, H.D., Michaels, A.F., 1993. Regional variability in size-fractionated C/<sup>234</sup>Th ratios in the upper ocean: importance of biological recycling. The Oceanography Society, Seattle, WA.
- Moran, S.B., Weinstein, S.E., Edmonds, H.N., Smith, J.N., Kelly, R.P., Pilson, M.E.Q., Harrison, W.G., 2003. Does <sup>234</sup>Th/<sup>238</sup>U disequilibrium provide an accurate record of particulate organic carbon export flux from the upper ocean? *Limnology and Oceanography* 48 (3), 1018–1029.
- Murray, J.W., Downs, J.N., Stoms, S., Wei, C.L., Jannasch, H.W., 1989. Nutrient assimilation, export production and <sup>234</sup>Th scavenging in the eastern equatorial Pacific. *Deep Sea Research* 36, 1471–1489.
- Nodder, S.D., Waite, A.M., 2001. Is Southern Ocean organic carbon and biogenic silica export enhanced by iron stimulated increases in biological production? Sediment trap results from SOIREE. *Deep-Sea Research II* 48, 2681–2701.
- Panagiotopoulos, C., Sempéré, R., Obernosterer, I., Striby, L., Goutx, M., Wambeke, F.V., Gautier, S., Lafont, R., 2002. Bacterial degradation of large particles in the Southern Indian Ocean using in vitro incubations experiments. *Organic Geochemistry* 33 (8), 985–1000.
- Park, Y.H., Gamberoni, L., 1995. Large-scale circulation and its variability in the south Indian Ocean from TOPEX/POSEIDON altimetry. *Journal of Geophysical Research* 100 (12), 24911–24929.
- Park, Y.H., Gamberoni, L., 1997. Cross-frontal exchange of Antarctic Intermediate Water and Antarctic Bottom Water in the Crozet Basin. *Deep-Sea Research II* 44, 963–986.
- Park, Y., Gamberoni, L., Charriaud, E., 1993. Frontal Structure, Water Masses and Circulation in the Crozet Basin. *Journal of Geophysical Research* 98 (C7), 12361–12385.
- Park, Y.H., Leboucher, V., Pollard, R., Read, J., Fèvre, J.L., 2002. A quasi-synoptic view of the frontal circulation in the Crozet Basin during the Antares-4 cruise. *Deep Sea Research II* 49 (9–10), 1823–1842.
- Pilskaln, C.H., Trull, T.W., Treguer, P.J., 2003. Zonal variability in carbon export and mesopelagic remineralization in the Southern Indian Ocean sector: Synthesis and global implications, JGOFS Final Open Science Conference, Washington DC, USA.
- Rintoul, S.R., Trull, T.W., 2001. Mixed layer properties of the Subantarctic and Polar Front Zones south of Australia. *Journal of Geophysical Research* 106 (C12), 31447–31462.
- Roy-Barman, M., Chen, J.H., Wasserburg, G.J., 1996. <sup>230</sup>Th-<sup>232</sup>Th systematics in the Central Pacific Ocean: the sources and the fates of thorium. *Earth and Planetary Science Letters* 139, 351–363.
- Rutgers van der Loeff, M.M., Freidrich, J., Bathmann, U.V., 1997. Carbon export during the spring bloom at the Antarctic polar front, determined with the natural tracer <sup>234</sup>Th. *Deep Sea Research* 44, 457–478.
- Rutgers van der Loeff, M.M., Moore, W.S., 1999. Determination of natural radioactive tracers. In: Grasshoff, K., Ehrhardt, M., Kremling, K. (Eds.), *Methods of Seawater Analysis*. 3rd ed. Verlag Chemie, Weinheim, pp. 365–397. (Chapter 13)
- Rutgers van der Loeff, M.M., Buesseler, K.O., Bathmann, U.V., Hense, I., Andrews, J., 2002. Comparison of carbon and opal export rates between summer and spring bloom periods in the region of the Antarctic Polar Front, SE Atlantic. *Deep Sea Research II* 49 (18), 3849–3869.
- Schmidt, S., Andersen, V., Belviso, S., Marty, J.-C., 2002. Strong seasonality in particle dynamics of north-western Mediterranean surface waters as revealed by <sup>234</sup>Th/<sup>238</sup>U. *Deep Sea Research I* 49 (8), 1507–1518.
- Sedwick, P.N., Blain, S., Quéguiner, B., Griffiths, F.B., Fiala, M., Bucciarelli, E., Denis, M., 2002. Resource limitation of

- phytoplankton growth in the Crozet Basin, Subantarctic Southern Ocean. *Deep Sea Research II* 49 (16), 3327–3349.
- Schiltzer, R., 2002. Carbon export fluxes in the Southern Ocean: results from inverse modeling and comparison with satellite-based estimates. *Deep Sea Research II* 49, 1623–1644.
- Trull, T., Bray, S., Manganini, S., Honjo, S., Francois, R., 2001. Moored sediment trap measurements of carbon export in the Sub-antarctic and Polar Frontal Zones of the Southern Ocean, south of Australia. *Journal of Geophysical Research* 106 (C12), 31489–31509.